DOI 10.1007/s11041-021-00650-4
Metal Science and Heat Treatment, Vol. 63, Nos. 1 – 2, May, 2021 (Russian Original Nos. 1 – 2, January – February, 2021)

TITANIUM ALLOYS

UDC 538.971:543.428.3:539.231

INVESTIGATION OF SURFACE LAYERS OF TITANIUM ALLOY VT6 WITH DEPOSITED CARBON FILM UNDER ION-BEAM STIRRING

N. M. Sozonova,[1] V. L. Vorob'ev,[1] F. Z. Gil'mutdinov,[1] M. I. Kazanbaev,[2] V. Ya. Bayankin,[1] and A. L. Ul'yanov[1]

Translated from *Metallovedenie i Termicheskaya Obrabotka Metallov*, No. 2, pp. 20 – 25, February, 2021.

The surface layer obtained by ion-beam stirring of a thin carbon film deposited on titanium alloy VT6 is studied. The composition and the chemical condition of elements in the surface layer are determined. Formation of a disordered carbon structure in a thin surface layer (20 – 40 nm) and of titanium carbides in the transition layer is detected. A model of formation of structure in the specimens during irradiation is developed. It is shown that formation of a disordered carbon structure, of titanium carbides, and of dislocation substructures is responsible for elevation of the microhardness of the specimens after ion-beam stirring.

Key words: ion-beam stirring, titanium carbides, disordered carbon, titanium alloy VT6, x-ray photoelectron spectroscopy, simulation.

INTRODUCTION

Modification of materials by ion beam stirring is an effective means for changing the structure and properties of metals and alloys [1, 2]. The properties of the surface layers of materials are very important, because they determine many characteristics including wear, corrosion and fatigue resistances [3, 4].

Deposition of surface layers based on carbides of transition metals, titanium carbides in particular, is used in machine building for improving the characteristics of the material and the appearance of the articles from them [5, 6]. Creation of multilayer coatings produces surface layers with various properties and good adhesion to the substrate.

The aim of the present work was to study the special features and mechanisms of formation of a surface carbon layer on alloy VT6 obtained with the use of ion beam treatment.

METHODS OF STUDY

We prepared specimens of titanium alloy VT6 shaped as plates with a size of 2 × 10 × 10 mm. VT6 belongs to the Ti – Al – V system and is a very widely used alloy [7]. Aluminum in such alloys raises their strength and heat resistance, and vanadium raises the strength and the ductility. Prior to depositing a carbon film, the specimens were subjected to a 1-h recrystallization annealing. Their surface was "ion-cleaned" with argon at a beam energy of 1.8 keV, a beam current of 100 mA and etching time 20 min. Carbon atoms were deposited by the magnetron method using graphite targets in a "Katod-1M" facility in an argon medium at a substrate temperature of 250°C. The thickness of the deposited film was 60 – 70 nm.

The carbon film and the titanium alloy were stirred by implantation of Ar^+ ions in a periodic pulse mode with frequency 100 Hz, pulse duration 1 msec, starting ion energy 30 keV, current density in a pulse 3 mA/cm^2, and irradiation doses 1×10^7 and 4×10^{17} ion/cm^2. Several specimens of the titanium alloy were irradiated with Ar^+ ions without deposition of carbon film. The parameters of their irradiation were the same as in the case of stirring carbon films at a dose of 1×10^{17} ion/cm^2.

To simplify the description of the results, we used the following notation: VT6 for the initial specimen, $Ar_2^+ \rightarrow$ VT6 for the specimen irradiated with Ar^+ ions in a dose of 1×10^{17} ion/cm^2; C/VT6 for the specimen with deposited carbon film; $Ar_1^+ \rightarrow$ C/VT6 and $Ar_2^+ \rightarrow$ C/VT6 for

[1] Udmurt Federal Research Center of the Ural Branch of the Russian Academy of Sciences, Izhevsk, Russia (e-mail: sozonova@udman.ru).
[2] Udmurt State University, Izhevsk, Russia.

the specimens with deposited carbon film after stirring with Ar^+ ions in a dose of 1×10^{17} and 4×10^{17} ion/cm^2, respectively.

The microhardness of the specimens was measured with the help of a PMT-3M microhardness meter according to the GOST 2999–75 Standard at a load of 1.2 N on the indenter with a hold for 10 sec under the load. The depth of the indent was 2.2 – 3.0 μm. In order to raise the reliability of the data obtained, the microhardness was measured for at least 20 times for each condition studied. Then we calculated the average value of the microhardness and its standard deviation.

The elements and the chemical condition of each element in the surface layers were studied by x-ray photoelectron spectroscopy (XRPS) using a SPECS spectrometer in magnesium K_α radiation (1253.6 eV). The layer-after-layer chemical composition was determined after etching the surface with argon ions with energy 4 keV and current density 30 μA/cm^2. The speed of the etching of the surfaces was about 1 nm/min. The relative error in the determination of the concentration of the elements was ± 3 at.% of the quantity measured.

The Raman spectra of the films were obtained using a HORIBA Jobyn Yvon HR800 spectrometer employing a helium laser (λ_{ex} = 632.8 nm) and an objective with 100-fold magnification. The diameter of the laser beam was 5 μm, the time of the exposure was 5 sec. The x-ray diffraction studies were performed with the help of a DRON-3M diffractometer in monochromatic copper K_α radiation. The x-ray phase analysis and the precision determination of the lattice parameters were conducted using a software for full-profile analysis [8] with allowance for all the reflections in an angle range 2θ from 20 to 130°. To determine the grain size and the sizes of the microdistortions, we used a modified method of Warren–Averbach harmonic analysis with approximation of the shape of the diffraction line by the Voigt function [9]. The method works with one reflection of the diffraction pattern and of the standard chosen for the analysis.

The simulation was conducted using the LAMMPS software [10] for classical molecular dynamics. Molecular dynamics makes it possible to trace the evolution of the interacting atoms in time by integrating the equations of motion. To study the surface layer, we created a random system with linear sizes $3.5 \times 3.5 \times 60$ nm containing at most 60,000 atoms. The harmonic boundary conditions were specified over three directions. For stabilization, the system obtained was exposed for 0.5 nsec to a temperature of 27°C using an NPT ensemble. Then we specified the conditions for relaxation of the system in the form of an NVE ensemble without controlling the temperature, and the system relaxed for 1 psec.

RESULTS AND DISCUSSION

In the initial condition, the specimens had a hardness of about 320 MPa (see Table 1).

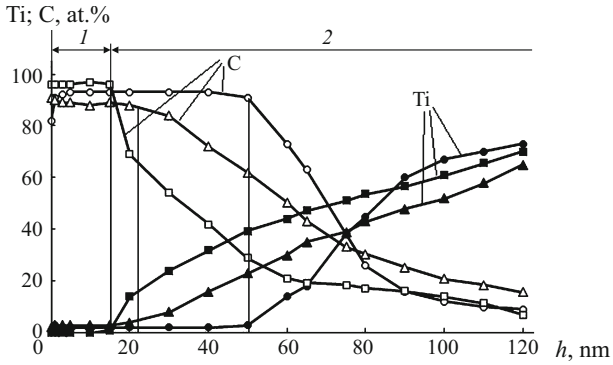

Fig. 1. Distribution of elements in surface layers of specimens of titanium alloy VT6: ○, ●) after sputtering of a carbon film (C/VT6); □, ■) after ion beam stirring with irradiation dose 1×10^{17} ion/cm^2 ($Ar_1^+ \rightarrow$ C/VT6); △, ▲) after ion beam stirring with irradiation dose 4×10^{17} ion/cm^2 ($Ar_2^+ \rightarrow$ C/VT6).

After the deposition of the carbon film, the microhardness of the specimens remained invariable within the measurement error. Ion beam stirring of the carbon film with irradiation doses 1×10^{17} and 4×10^{17} ion/cm^2 raised the microhardness by 137 and 198%, respectively.

The XRPS study before and after the ion beam stirring showed that the subsurface layer with carbon could be divided into two layers (Fig. 1). Layer *1* consisted chiefly of carbon, and layer *2* was a transition one from the carbon layer to the substrate. The carbon concentration in the transition layer started to decease, while that of titanium and of the alloying elements started to in increase. The content of the alloying elements (Al and V) in the transition layer did not exceed their concentration in the volume. The distribution of elements in the specimens after the stirring and sputtering of the carbon film differed, i.e., the thickness of layer *1* decreased and that of layer *2* increased (Fig. 1). For example, the thickness of layer *1* in the $Ar_2^+ \rightarrow$ C/VT6 specimen decreased from 50 to 20 nm, and the thickens of the transition layer increased from 70 to 120 nm and even more. This may be explained by sputtering of the carbon films under the bombardment with Ar^+ ions and mixing of the sputtered carbon with the atoms of the target due to formation of cascades of atomic collisions.

TABLE 1. Average Microhardness (*HV*) of Surface Layers, its Standard Deviation (Δ), and Sizes of Regions of Coherent Scattering (RCS) of Specimens of Alloy VT6 in Different States

Specimen	*HV*, MPa	Δ, MPa	RCS, nm
VT6	320	32	48
C/VT6	288	40	48
$Ar_1^+ \rightarrow$ C/VT6	684	62	35
$Ar_2^+ \rightarrow$ C/VT6	860	58	36

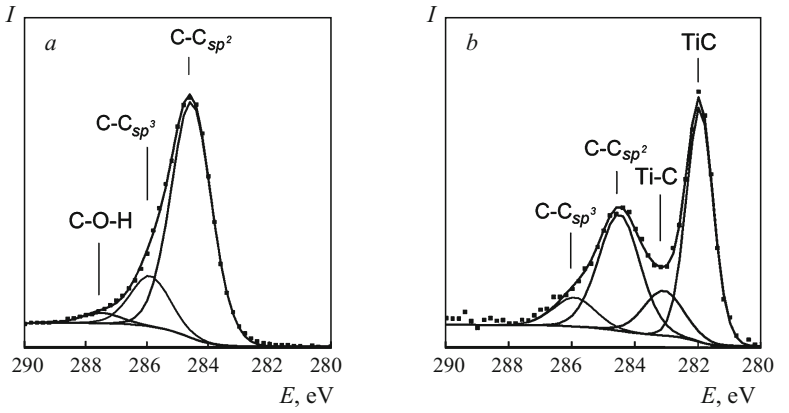

Fig. 2. C1s spectra at a distance of about 30 nm (*a*) and about 90 nm (*b*) from the surface of alloy VT6 with sputtered-on carbon film after ion beam stirring (specimen $Ar_I^+ \rightarrow C/VT6$).

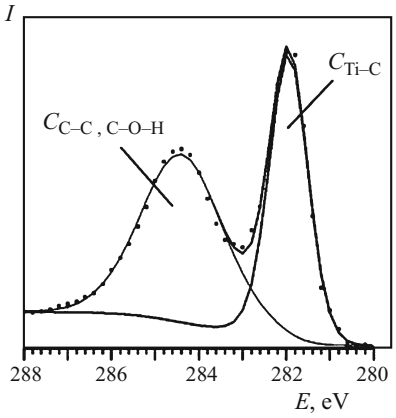

Fig. 3. C1s spectrum obtained from specimen $Ar_I^+ \rightarrow C/VT6$ of alloy VT6 with sputtered-on carbon film after ion beam stirring with irradiation dose 1×10^{17} ion/cm^2 at a distance of about 90 nm from the surface as decomposed into two constituents.

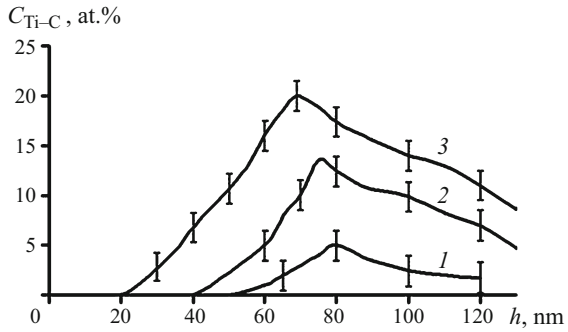

Fig. 4. Concentration profiles of the distribution carbon with Ti–C-bonds over the thickness of specimens (*h* is the distance from the surface) in the initial film (*1*) and after stirring with irradiation doses 1×10^{17} (*2*) and 4×10^{17} ion/cm^2 (*3*).

Analysis of the x-ray photoelectron spectra C1s has shown that carbon is present in layer *1* in three states both after the sputtering and after the ion beam stirring (Fig. 2*a*). The first state (the dominant one) is represented by C–C-bonds with sp^2-hybridization of the valence electrons (E_b = 284.6 eV). The second state is represented by C–C-bonds with sp^3-hybridization of the valence electrons (E_b = 286 eV), and the third state is represented by carbon with C–O–H-bonds (E_b = 287 – 289 eV). Ion irradiation should be accompanied by disordering of the carbon structure, but we could not detect the difference from the C1s XRPS spectra in the first layer of the specimens before and after the stirring. The transition layer has two more states of carbon with bonding energy 282 eV and 283.1 eV in addition to the three mentioned ones (Fig. 2*b*). Most probably, both these states correspond to carbon in the Ti–C-bonds [11]. We may expect formation a TiC titanium carbide or of carbides with an intermediate composition like Ti_8C_{12} or with a nonstoichiometric proportion of the components.

If we describe the C1s spectrum in the transition layer by only two constituents, as it is shown in Fig. 3, we will be able to asses qualitatively the concentration of carbon spent for formation of titanium carbides. This means that we will assess qualitatively the content of titanium carbides in the transition layer of the specimens. The results of such calculation are presented in Fig. 4. The content of titanium carbides in the transition layer after ion beam stirring attains 20 at.% (curve *3* in Fig. 4), whereas in the initially sputtered film it does not exceed 5 at.% (curve *1* in Fig. 4). This means the ion beam stirring creates conditions for formation of titanium carbides on the surface of the titanium alloy in the transition layer between the film and the substrate. We may assume that the formation of titanium carbides in the transition layer after ion beam stirring is one of the causes of growth in the microhardness of the alloy.

The study of the Raman spectra has shown that the Raman spectrum of the initially sputtered film consists of two strongly smeared bands *D* with $\Delta\nu \sim 1375$ cm^{-1} and *G* with $\Delta\nu \sim 1582$ cm^{-1} (Fig. 5). By the data of [12], peak *G* corresponds to carbon with a structure of graphite, i.e., to carbon with an sp^2-hybridization of the valence electrons, while the presence of peak *D* corresponds to a disordered state of carbon. It can be seen from Fig. 5 that after the sputtering of the carbon film, the intensities of peaks *G* and *D* are commensurable. This means that the structure of carbon in the initially sputtered film is disordered. After the ion beam

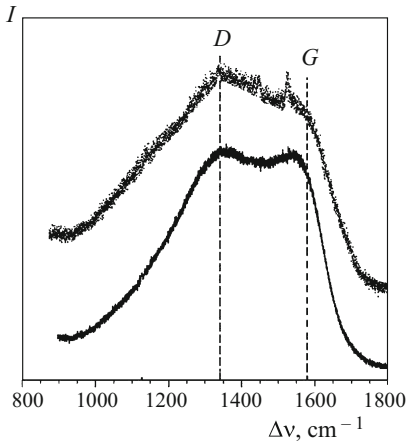

Fig. 5. Raman spectra of the initial carbon film (*1*) and of the film after ion beam stirring with irradiation dose 1×10^{17} ion/cm^2 (*2*).

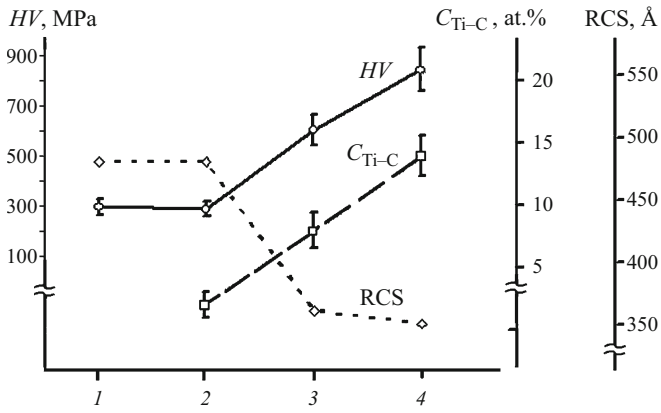

Fig. 6. Joint plot of variation of microhardness (*HV*), concentration of carbon participating in the Ti–C bonds ($C_{Ti–C}$), and RCS in different stages of formation of carbon layer in alloy V6: *1*) VT6; *2*) C/VT6; *3*) $Ar_1^+ \rightarrow$ C/VT6; *4*) $Ar_2^+ \rightarrow$ C/VT6.

stirring, peak *D* becomes more intense than peak *G.* There is virtually no gap between the peaks (Fig. 5). We may state that after the stirring carbon becomes more disordered, which may be an indirect indication of formation of titanium carbides in the transition layer.

The x-ray spectrum analysis has not shown difference in the phase compositions of the specimens before and after the ion beam stirring; the dominant phase is α-Ti with a hcp lattice. At the same time, the computation of the regions of coherent scattering (RCS) has shown that the specimens after the ion beam stirring of carbon exhibit lower coherent scattering (see Table 1), i.e., from 48 nm in the initial specimen to 35 – 38 nm after the stirring. This may be associated with generation of dislocations and formation of dislocation substructures under the conditions of ion beam stirring [13, 14]. It has been shown in [13, 14] that ion irradiation of annealed metals causes structural and phase changes in the surface layer due to generation of dislocations and subsequent formation of dislocation structures. It is possible that the reduction of the RCS under ion beam stirring of carbon is also connected with this very process.

If we impose the results obtained by different methods and by measurement of microhardness in one plot, we will see their correlation (Fig. 6). The growth in the microhardness of the specimens after the ion beam stirring of carbon is accompanied by growth in the concentration of titanium carbides in the transition layer and reduction of the RCS. The growth in the microhardness reflects hardening of the surface layer. In its turn, the strengthening of the surface is a result of formation of titanium carbides in the transition layer and of dislocation substructures outside the range of penetration of the alloying admixture.

The changes in the structure of the initial alloy due to ion beam stirring require a detailed study in different scale levels. Computer simulation is an effective approach to investigation of various changes in a substance. A theoretical approach makes it possible to analyze the atomic structures and the laws of their spatial and time transformations.

Computations within molecular dynamics represent the main properties of materials accurately enough, but depend substantially on the choice of the potential describing the interaction between particles. To create a steady disordered system, we used the Tersoff potential for carbon [15]. The computed density of the structure obtained was 2.13 g/cm^3. The structures were visualized with the help of the OVITO software [16] designed for structural analysis and plotting of graphs in molecular dynamic simulation.

We simulated irradiation of disordered carbon with an argon atom using a hybrid potential consisting of the Tersoff potential for carbon [10] and the universal Ziegler – Biersack – Littmark (ZBL) potential [17]. To compute the potential energy of the interaction between carbon atoms and an argon ion, we used the ZBL potential, which has the form of a screened Coulomb interaction and characterizes the repulsion of a positively charged ion from carbon atoms.

To integrate the equations of motion, with used the Verlet algorithm [10] and chose a constant time step $dt = 5 \times 10^{-15}$ sec for stability of the solution of the dynamics equations.

Figure 7 presents the initial condition of the simulation. The argon atom is located at a distance of 0.5 nm from the center of the surface of the specimen, which exceeds the cutoff radius of the used potential. The angle of input of the ion into the specimen is 90°. The initial energy of the incoming argon ion in accordance to the experimental value was chosen to be equal to 30 keV.

Ion beam stirring occurs through multiple shifts of the atoms of the specimen triggered by one ion. The primary knocked-on atom continues to collide with other atoms triggering secondary collisions. Such multiple shifts are called a cascade of atomic collisions [18].

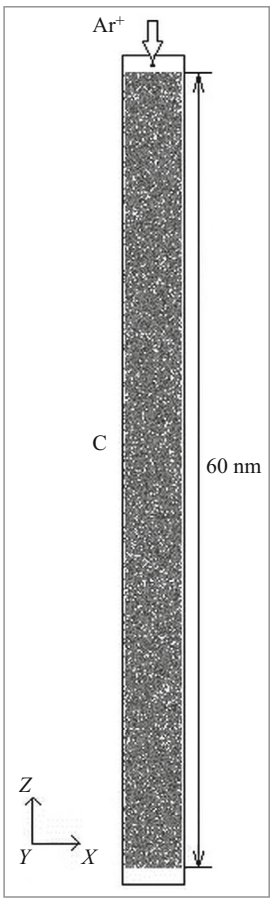

Fig. 7. Model of disordered carbon layer (C) with initial location of argon ion (Ar^+). The arrow points in the direction of the motion of the argon ion. The thickness of the carbon film is 60 nm.

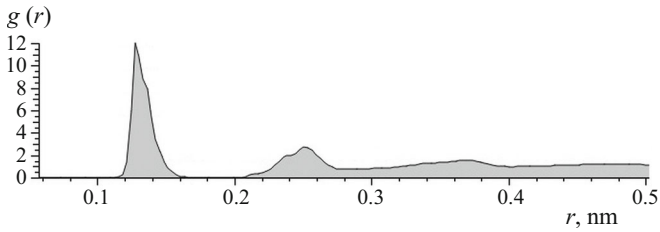

Fig. 9. Function $g(r)$ of radial distribution of carbon atoms after irradiation with argon ion.

Processing of the results of the simulation revealed knocking of atoms from the surface (Fig. 8*a*) and start of formation of a cascade of atomic collisions in the volume of carbon (Fig. 8*b*). The depth of penetration of the argon ion into the specimen was computed to be ~ 35 nm. This indicates that such ions reach the transition region and are able to create conditions for formation of titanium carbides due to appearance of cascades of atomic collisions. The atoms sputtered from the surface of the material are marked in Fig. 8*a*.

Figure 9 presents the function of radial distribution of atoms of the carbon layer after irradiation. Analysis of the function of radial distribution of carbon atoms in the initial and irradiated film shows that the structure of the film does not change substantially. The film preserves the structure of disordered substance, which is confirmed by splitting of the second maximum of the function of radial distribution [19].

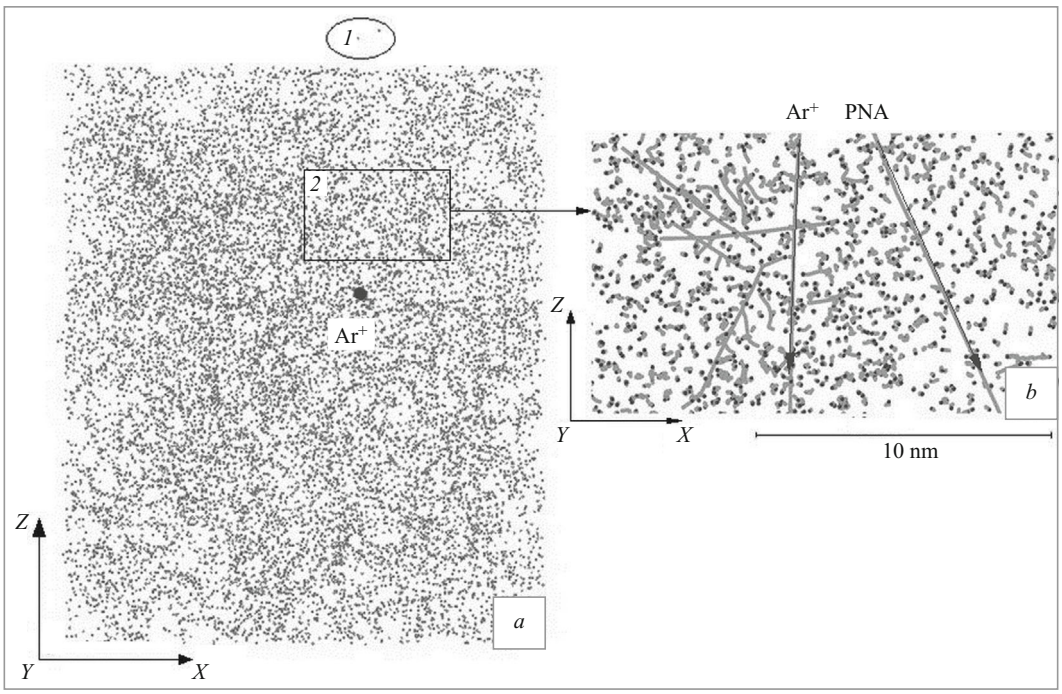

Fig. 8. Results of simulation of the system of a disordered carbon film under irradiation with argon ion: *a*) general view (the atoms sputtered from the surface of the film are depicted in region *1*); *b*) magnified region *2* with trajectories of each atom (the gray lines); the arrows present the trajectories of the motion of the argon ion (Ar) and of the primary knocked atom (PNA).

CONCLUSIONS

The results of the study show that ion beam stirring of carbon on the surface of titanium alloy VT6 yields a disordered carbon structure with dominant sp^2-hybridization of the C–C-bonds, titanium carbides in the transition layer, and dislocation substructures. By the data of the computer simulation, carbon atoms are knocked from the surface of the film producing cascades of atomic collisions and permeation of argon atoms to a depth of about 35 nm. The formation of a disordered carbon structure, titanium carbides and dislocation substructures is responsible for growth in the microhardness of the specimens after ion beam stirring.

To continue the present work, we plan to study the processes of ion beam stirring on the 'film – titanium alloy' interface by the method of molecular dynamics.

The work has been performed with the use of the equipment of the common access "Center for Physical and Physicochemical Methods of Analysis, Investigation of Properties and Characteristics of Surface, Nanostructures, Materials and Articles" of the Udmurt Research Center of the Ural Branch of the Russian Academy of Sciences within State Assignment of the Ministry of Science and Higher Education of the Russian Federation (Reg. No. AAAA-A17-117022250040-0).

REFERENCES

1. B. A. Kalin, N. V. Volkov, and I. B. Oleinikov, "Stirring in multilayer films and alloying of near-surface layers of polycrystalline substrates under the impact of ion beams with wide energy spectrum," *Izv. Ross. Akad. Nauk, Ser. Fiz*., **76**(6), 771 – 776 (2012).
2. F. F. Komarov, V. M. Konstantinov, A. V. Kovalchuk, et al., "The effect of steel substrate pre-hardening on structural, mechanical, and tribological properties of magnetron sputtered TiN and AlN coatings," *Wear*, **352 – 353**, 92 – 101 (2016).
3. I. V. Ivanov, A. Thoemmes, V. Yu. Skiba, et al., "Effect of the power density of electron beam on the structure of titanium under out-of-vacuum electron-beam treatment," *Metalloved. Term. Obrab. Met*., No. 10, 10 – 17 (2018).
4. J. Mackerle, "Coatings and surface modification technologies: a finite element bibliography (1995 – 2005)," *Model. Simul. Mater. Sci. Eng*., No. 13, 935 – 979 (2005) (doi: 10.1088/0965-0393/13/6/011).
5. V. I. Kalita, D. I. Komlev, G. A. Pribytkov, et al., "Structure, phase composition and microhardness of a plasma cermet TiC – Ti coating," *Fiz. Khim. Obrab. Mater.*, No. 3, 16 – 28 (2018).
6. A. Rajabi, M. J. Ghazali, and A. R. Daud, "Chemical composition, microstructure and sintering temperature modifications on mechanical properties of TiC-based cermet — A Review," *Mater. Design*, **67**, 46 – 95 (2915).
7. R. Hauert and J. Patscheilder, "From alloying to nanocomposites — improved performance of hard coatings," *Adv. Eng. Mater.*, **2**(5), 247 – 259 (2000).
8. N. P. D'yakonova, E. V. Shelekhov, T. A. Sviridova, and A. A. Reznikov, "Quantitative x-ray phase analysis of weakly textured objects," *Zavod. Lab*., **63**(10), 17 – 24 (1997).
9. G. A. Dorofeev, A. N. Streletskii, I. V. Povstugar, et al., "Determination of the sizes of nanoparticles of x-ray diffractometry," *Kolloid. Zh*., **74**, 710 – 720 (2012)
10. URL: http://lammps.sandia.gov/.
11. C. D. Wagner, W. M. Rigus, and L. E. Davis, *Handbook of X-Ray Photoelectron Spectroscopy*, Physical Electronics Div., Perkin-Elmer Corp., Eden Prairie (1979).
12. A. C. Ferrari and J. Robertson, "Raman spectroscopy of amorphous, nanostructured, diamond-like carbon, and nanodiamond.," *Phil. Trans. R. Soc. London*, **A362**, 2477 – 2512 (2004).
13. A. P. Gulyaev, *Metal Science* [in Russian], Metallurgiya, Moscow (1986), 544 p.
14. I. A. Kuzina, E. V. Kozlov, and Yu. P. Sharkeev, *Gradient Surface Layers Based on Intermetallic Particles* [in Russian], Izd. NTL, Tomsk (2013), 260 p.
15. L. Lindsay and D. A. Broido, "Optimized Tersoff and Brenner empirical potential parameters for lattice dynamics and phonon thermal transport in carbon nanotubes and graphene," *Phys. Rev. B*, **81**, 205441 (2010).
16. URL: https://ovito.org/index.php/.
17. J. F. Zeigler, J. P. Biersack, and U. Littmark, *The Stopping and Range of Ions in Solids*, Pergamon, New York (1985), 321 p.
18. F. F. Komarov, A. P. Novikov, and A. F. Burenkov, *Ion Implantation* [in Russian], Izd. "Universitetskoe," Minsk (1994), 303 p.
19. V. P. Voloshin and Yu. I. Naberukhin, "On the origin of splitting of second maximum in the radial distribution function of amorphous solids," *Zh. Strukt. Khim*., **38**(1), 78 – 88 (1997).